

# UV-VIS optical spectroscopy investigation on the kinetics of long-lived RONS produced by a surface DBD plasma source

E. Simoncelli<sup>1</sup>, J. Schulpen<sup>2</sup>, F. Barletta<sup>1</sup>, R. Laurita<sup>1</sup>, M. Gherardi<sup>1,3</sup>, V. Colombo<sup>1,3</sup> and A. Nikiforov<sup>4</sup>

<sup>1</sup>Department of Industrial Engineering, Alma Mater Studiorum-Università di Bologna, Bologna, Italy

<sup>2</sup>Eindhoven University of Technology, Eindhoven, Netherlands

<sup>3</sup>Industrial Research Center for Advanced Mechanics and Materials, Alma Mater Studiorum-Università di Bologna, Bologna, Italy

<sup>4</sup>Department of Applied Physics, Ghent University, Ghent, Belgium

**Abstract:** This work aims at investigating, by means of UV-Vis spectroscopic techniques, the kinetics of O<sub>3</sub>, NO<sub>2</sub> and NO<sub>3</sub> produced by a Surface Dielectric Barrier Discharge. The phenomenon of discharge poisoning (or *ozone quenching*) in static air was investigated varying the electrical power density associated with the plasma source. Moreover, considerations on the production of NO, one of the most relevant the O<sub>3</sub>-quenchers, are drawn upon measurements of the N<sub>2</sub> vibrational temperature.

**Keywords:** SDBD, optical spectroscopy, RONS kinetics, discharge poisoning.

## 1. Introduction

The knowledge of the gas phase chemistry of a cold atmospheric plasma (CAP) is a fundamental step for a more thorough understanding of the effects that can be induced in gas phase or on substrates. This work aims at investigating, by means of optical spectroscopic techniques, the kinetics of long-lived reactive oxygen and nitrogen species (RONS) produced by a Surface Dielectric Barrier Discharge (SDBD). Literature regarding ozone production technologies reports that DBDs operating in air at low power densities (<0,2 W/cm<sup>2</sup>), produce an ozone dominated atmosphere [1–5]; while at high power densities the evolution in time from an ozone enriched atmosphere to a NO<sub>x</sub> enriched one is observed due to the so-called discharge poisoning [2,3]. Although many different scientific studies investigated the gas phase average concentration of CAP-derived RONS [1,4], only few were performed with the aim of investigating RONS kinetics [5]. Following these considerations, in this work the effects of discharge poisoning were studied through the measurements of the kinetics of O<sub>3</sub>, NO<sub>2</sub> and NO<sub>3</sub> produced by a SDBD working in static air at different applied power densities, using a procedure based on optical absorption spectroscopy (OAS). Moreover, since the production of NO, one of the most important quenchers of O<sub>3</sub>, is supposed to be strictly affected by the vibrational excitation of the ground state of nitrogen molecules [2], the vibrational temperature of N<sub>2</sub> was determined by processing optical emission spectroscopy (OES) data.

## 2. Materials & Methods

The surface DBD source adopted in this study (Fig.1) was designed to create a confined volume with optical accesses (three quartz windows) for UV-VIS spectroscopy and absorption measurements. The source was composed of a mica dielectric layer (2 mm thick) interposed between

an air-cooled high voltage (HV) aluminium electrode and a grounded electrode (AISI 316L rhomboid mesh), forming the surface DBD source. The device, operating in environmental air, was driven by a micropulsed generator (AlmaPULSE, AlmaPlasma srl, Italy); the discharge time, determined as the time in which the generator was set on for 90 seconds for all investigated cases. To evaluate the surface power density (SPD) associated with the plasma source, voltage and current waveforms were recorded by means of a high voltage probe (Tektronix P6015A) and a current probe (Pearson 6585) connected to an oscilloscope (Tektronix DPO40034). The plasma source was operated at different values of SPD, varying voltages from 4 kV to 11 kV with 1 kV increments, with fixed frequency (10 kHz) and duty cycle (DC=100%) for both OAS and OES measurements.

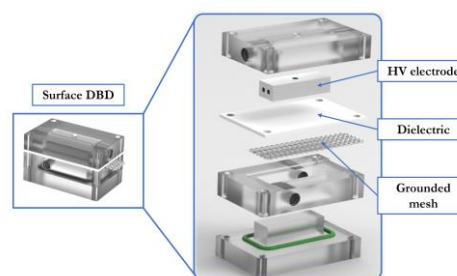


Figure 1. 3D schematic of surface DBD plasma source used in the experimental activities.

The setup for absorption spectroscopy, shown in Fig.2, was composed by a broad band spectrum lamp, an optical setup to investigate the region under the mesh of the SDBD, a spectrometer (Acton SP2500i, Princeton Instruments) and a photomultiplier tube (PMT-Princeton Instruments PD439) connected to a wideband oscilloscope (Tektronix DPO40034) as detector.

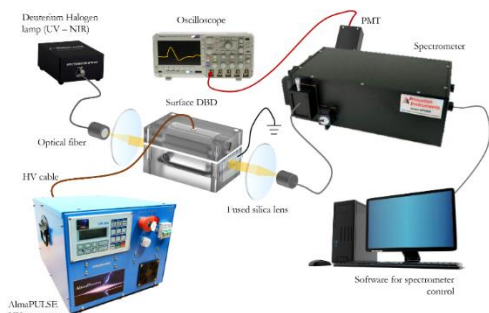


Figure 2. Schematic of the experimental setup for optical absorption spectroscopy.

In order to quantitatively evaluate the species concentrations from absorption measurements, the Lambert-Beer law has to be taken into account. Considering simultaneously the absorption contributions of the investigated species ( $i$ -species) at different wavelengths ( $j$ -wavelength), the following linear system is obtained:

$$\begin{bmatrix} \sigma_{11} & \dots & \sigma_{1N} \\ \vdots & \ddots & \vdots \\ \sigma_{N1} & \dots & \sigma_{NN} \end{bmatrix} \begin{pmatrix} n_1 \\ \vdots \\ n_N \end{pmatrix} = -\frac{1}{L} \begin{pmatrix} A_1 \\ \vdots \\ A_N \end{pmatrix} \quad (1)$$

Where  $\sigma_{i,j}$  represents the absorbing cross section of the  $i$ -species at  $\lambda_j$ ,  $n_i$  is the average density of the  $i$ -species,  $L$  is the optical path of the system, and  $A_j$  is the absorbance at the  $j$ -wavelength.

For the measurements of  $O_3$ ,  $NO_2$  and  $NO_3$  kinetics, the matrix of absorption cross sections  $[\sigma_{i,j}]$  was defined according to procedure exposed by Moiseev [6] and the profiles  $\sigma(\lambda)$  were taken from the MPI-Mainz UV/VIS Spectral Atlas database ([satellite.mpic.de/spectral\\_atlas](http://satellite.mpic.de/spectral_atlas)).

Regarding the OES measurements, the plasma emission was collected through a quartz window positioned at the bottom of source by means of an optical fibre and the same spectrometer as used for OAS experiments. Emission spectra of the second positive system  $N_2(C^3\Pi_u \rightarrow B^3\Pi_g)$  in the range 300-450 nm were acquired to determine the vibrational temperature ( $T_{vib}$ ) of the  $N_2$  molecule. An estimation of the  $T_{vib}$  of  $N_2$  molecules was obtained applying the Boltzmann plot method to the emission spectra [7].

### 3. Results

The kinetics of ozone for the investigated SPDs are shown in Fig. 3. At low SPDs ( $SPD \leq 0,11 \text{ W/cm}^2$ ),  $O_3$  concentration shows a continuous increase during the discharge time: the higher is the SPD, the higher is the ozone concentration reached at the end of the discharge time. For values of SPD above  $0,11 \text{ W/cm}^2$ , ozone concentration reaches a maximum and then decrease, revealing the ozone quenching phenomenon. The higher the SPD, the earlier the ozone quenching phenomenon appears.

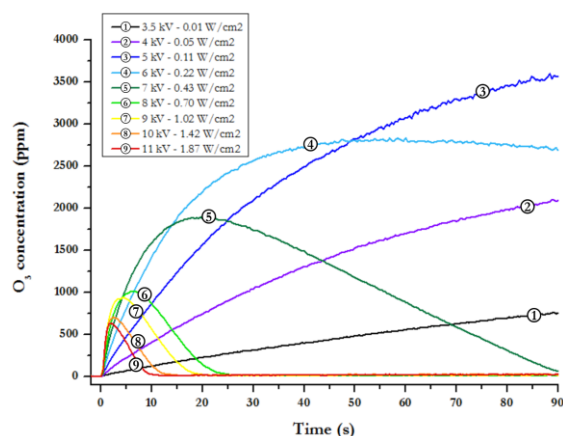


Figure 3. Kinetics of  $O_3$  concentration produced during 90 sec of discharge using different SPDs ( $0,01 - 1,87 \text{ W/cm}^2$ ).

The kinetics of  $NO_3$  depending on the SPD in the range between  $0,01 - 1,89 \text{ W/cm}^2$ , is shown in Fig. 4. The results underline that the temporal profiles of  $NO_3$  concentration are qualitatively similar to the ozone's ones.

The measured  $NO_2$  kinetics for different SPDs ( $0,01 - 1,87 \text{ W/cm}^2$ ) are presented in Fig. 5, considering up to 90 sec of discharge time. Unlike what seen for  $O_3$  and  $NO_3$  concentrations,  $NO_2$  molecules are detectable only working with SPDs higher than  $0,22 \text{ W/cm}^2$ , which incidentally is the minimum value of SPD for which the  $O_3$  quenching was observed.

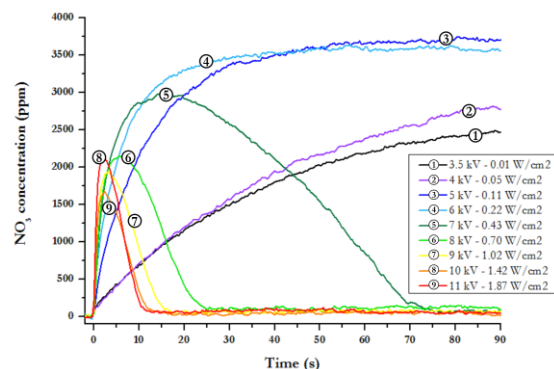


Figure 4. Kinetics of  $NO_3$  concentration produced during 90 sec of discharge time using different SPDs ( $0,01 - 1,87 \text{ W/cm}^2$ ).

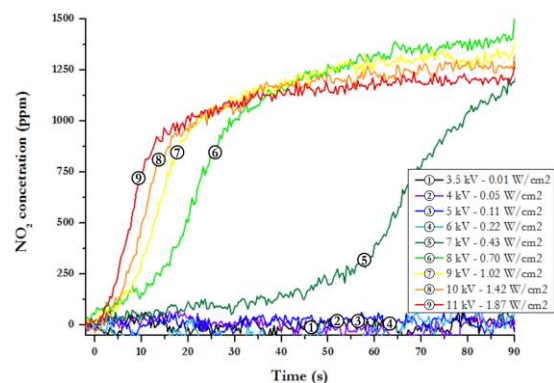


Figure 5. Kinetics of NO<sub>2</sub> density produced during 90 sec of discharge time using different SPDs (0,01 – 1,87 W/cm<sup>2</sup>).

The values of T<sub>vib</sub> of N<sub>2</sub><sup>\*</sup>, plotted in Fig. 6 as a function of SPD, reveal a monotonous increase of T<sub>vib</sub> as a function of the SPD. Vibrational temperatures higher than 5000 K are found to be associated to SPDs for which the ozone quenching was experimentally observed (SPD > 0,22 W/cm<sup>2</sup>).

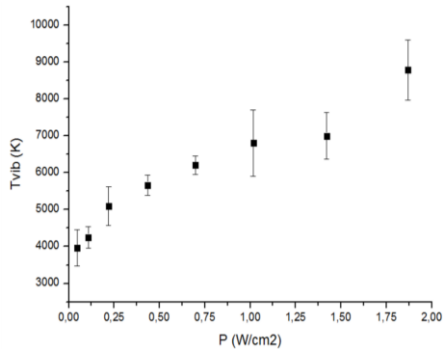


Figure 6. Values of T<sub>vib</sub> of N<sub>2</sub><sup>\*</sup> measured for different SPDs by means of OES technique. Frequency: 10 kHz, Duty Cycle: 100%.

#### 4. Discussion

Differently from oxygen-fed ozonisers, in air plasmas the production-destruction cycle of ozone is affected by the presence of nitrogen molecules. Several gas-phase reactions between charged, excited and neutral species take place simultaneously in the plasma and afterglow regions involving different RONS such as ozone (O<sub>3</sub>), nitrogen oxides (N<sub>x</sub>O<sub>y</sub>) and nitroxyl/nitrous/nitric acids (HNO, HNO<sub>2</sub>, HNO<sub>3</sub>). The main reaction (production and depletions reactions) involving O<sub>3</sub>, NO<sub>3</sub> and NO<sub>2</sub> are reported in Table.1.

Table 1. Main reactions involving O<sub>3</sub>, NO<sub>3</sub>, NO<sub>2</sub> [8].

Main reactions	
R1	$O + O_2 \rightarrow O_3$
R2	$O_3 + N \rightarrow NO + O_2$
R3	$O_3 + NO \rightarrow NO_2 + O_2$
R4	$O_3 + NO_2 \rightarrow NO_3 + O_2$
R5	$NO_2 + O \rightarrow NO_3$
R6	$NO_2 + O \rightarrow NO + O_2$

As shown in Fig. 3, in the first few seconds of the discharge time an increase of SPD always leads to an increase of the ozone production rate, due to the production rate of the O atom being directly proportional to the SPD [10]. When a SPD > 0,22 W/cm<sup>2</sup> is applied to the discharge working in air, the ozone quenching is observed. Several studies on air ozonisers [4,9,10] and on air micro-discharges [2] suggest that this phenomenon is caused by an increase of the amount of nitrogen oxides. As a matter of fact, in the case of air plasma, when the concentration of NO<sub>x</sub> (NO and NO<sub>2</sub>) exceeds the threshold value around 0,03%, the main contribution in the destruction of ozone is

given by NO<sub>x</sub> molecules through different reactions such as R3 and R4 [2].

Fig.7 shows O<sub>3</sub> and NO<sub>2</sub> kinetics for low (0,11 W/cm<sup>2</sup>) and high (1,42 W/cm<sup>2</sup>) values of SPD: for SPD = 0,11 W/cm<sup>2</sup> ozone concentration steadily increases while NO<sub>2</sub> remains undetectable; on the other hand, at SPD = 1,42 W/cm<sup>2</sup>, NO<sub>2</sub> firstly reacts with O<sub>3</sub> and O following the reactions R4, R5 and R6 and then, when the O<sub>3</sub> concentration drops, NO<sub>x</sub> starts to raise and accumulate, resulting in a fast increase of its concentration during the discharge poisoning. As well noticeable comparing Fig. 3 and Fig. 5, the higher the SPD, the earlier the discharge poisoning effect, resulting in the NO<sub>2</sub> concentration build-up, takes place.

The reaction pathway, composed by reactions R2, R3 and R4, ends with the formation of NO<sub>3</sub> molecule. At low SPDs (SPD < 0,11 W/cm<sup>2</sup>), ozone is partially consumed by the above-mentioned pathway, resulting in the increase of NO<sub>3</sub> concentration that is accumulated in time. Differently, for the SPDs for which discharge poisoning occurs (SPD > 0,22 W/cm<sup>2</sup>), the quenching of ozone leads to the decay of NO<sub>3</sub> concentration.

As described above, the discharge poisoning effect can be considered a threshold phenomenon, associated to a fast increase of concentration of the ozone-quencher NO molecule [2,3] that can rapidly react with ozone to form NO<sub>2</sub> through reaction R3.

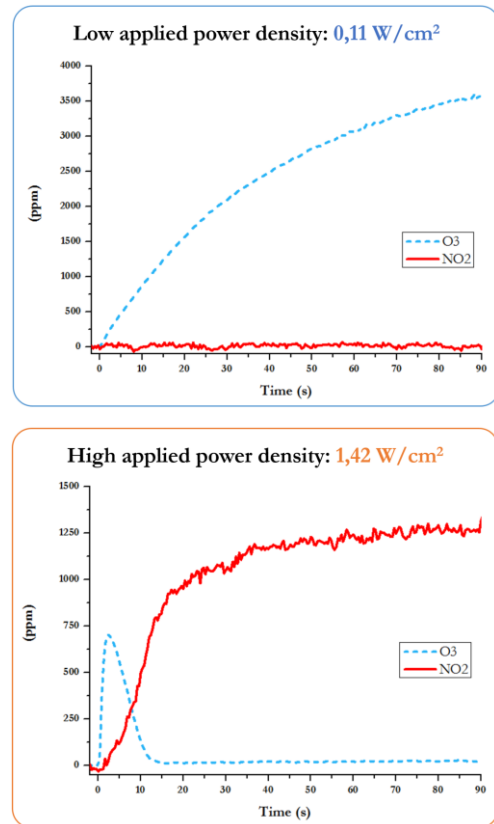


Figure 7. Comparison of kinetics profiles of O<sub>3</sub> and NO<sub>2</sub> densities for low (upper) and high (bottom) SPD.

Thus, the NO molecule and its relative production play important role in the discharge poisoning. It is worth underling that the process for direct NO synthesis is limited by the energy required for the breaking of the strong bond (10 eV) in the N<sub>2</sub> molecule. At high temperatures, the direct NO synthesis is obtained through the well-known Zeldovich mechanism. On the other hand, in low temperature non-equilibrium discharges other reactions based on the vibrationally excited population of N<sub>2</sub>, generally defined as N<sub>2</sub>(v), can support the synthesis of NO. In this frame, non-equilibrium plasmas offer an alternative and more efficient mechanism for N<sub>2</sub> dissociation based on both a direct and a stepwise electronic excitation sequence, resulting in an additional production of N atoms for the NO synthesis. The electrons impact to the neutral molecules promote the formation of highly vibrationally excited N<sub>2</sub> molecules in air through vibrational-vibrational (VV) exchanges, and, in turn, the formation of free N atoms, reactants for the direct production of NO molecules.

As reported by Fridman [2], the energy efficiency of NO production in air non-equilibrium plasma is greatly enhanced when the vibrational temperature (T<sub>vib</sub>) of N<sub>2</sub> is high enough to avoid the vibrational-translational (VT) relaxation [2].

Our measurements of nitrogen T<sub>vib</sub> highlight a monotonic relation between T<sub>vib</sub> and the source SPD (Fig. 6), with T<sub>vib</sub> reaching values over 5000 K for SPD > 0,22 W/cm<sup>2</sup>. This is the minimum SPD at which we observed the phenomenon of ozone quenching, supporting the idea that, after overcoming a critical value of T<sub>vib</sub> of N<sub>2</sub>, a stable production of NO molecules is established and provokes the discharge poisoning.

The experimental activity presented in this work is in the line of thought of using the results of OAS technique as an on-line monitoring system for the control of a plasma activated atmosphere. The possibility to monitor in real-time the kinetics of some relevant reactive species can pave the way for the development of a cost-effective system based on OAS diagnostic to be implemented in plasma-assisted industrial processes. Moreover, the characterization of gas phase by means of spectroscopy techniques can gain a deeper understating of the CAP-effects in biological applications, such as in the material treatments for microbial inactivation or surface activation, as a first step in correlating the chemistry in gas phase with the effects induced in the process target.

## 5. Conclusions

Optical absorption and emission spectroscopies were adopted in this experimental activity in order to investigate the discharge poisoning effect. Surface DBDs can activate air promoting an O<sub>3</sub>- or NO<sub>x</sub>-enriched atmosphere operating at low or high SPDs respectively. The experimental results proved that the ozone quenching effect behaves as a threshold phenomenon and it is observable for SPDs higher than 0,11 W/cm<sup>2</sup>. Moreover, the kinetics analysis highlighted the temporal evolution of

poisoning and how the chemical composition of the atmosphere changes in time. The measurements of vibrational temperature of nitrogen molecules supported the explanation of the ozone quenching stimulated by non-equilibrium vibrational excitation of N<sub>2</sub>: once a threshold value of vibrational energy (~ 5000 K) is overcome, NO synthesis becomes possible at low temperature and NO production rate increases significantly, resulting in the ignition of a strong ozone quenching.

Finally, the activity supported the idea to adopt and develop OAS diagnostic as on-line monitoring system for the control of plasma-assisted processes and optimization of plasma treatment for industrial and biomedical applications.

## 6. Acknowledgements

This work was partially supported by the COST Action TD1208: Electrical discharges with liquids for future applications.

## 7. References

- [1] U. Kogelschatz, *Plasma Chemistry and Plasma Processing* **23**, 1 (2003).
- [2] A. Fridman, *Plasma Chemistry* (2008).
- [3] T. Shimizu, Y. Sakiyama, D. B. Graves, J. L. Zimmermann, and G. E. Morfill, *New Journal of Physics* **14**, 103028 (2012).
- [4] U. Kogelschatz and P. Baessler, *Ozone: Science & Engineering* **9**, 195 (1987).
- [5] I. A. Kossyi, A. Y. Kostinsky, A. A. Matveyev, and V. P. Silakov, *Plasma Sources Science and Technology* **1**, 207 (1992).
- [6] T. Moiseev, N. N. Misra, S. Patil, P. J. Cullen, P. Bourke, K. M. Keener, and J. P. Mosnier, *Plasma Sources Science and Technology* **23**, 065033 (2014).
- [7] N. Masoud, K. Martus, M. Figus, and K. Becker, *Contributions to Plasma Physics* **45**, 32 (2005).
- [8] Y. Sakiyama, D. B. Graves, H.-W. Chang, T. Shimizu, and G. E. Morfill, *Journal of Physics D: Applied Physics* **45**, 425201 (2012).
- [9] S. Yagi and M. Tanaka, *Journal of Physics D: Applied Physics* **12**, 1509 (1979).
- [10] U. Kogelschatz, B. Eliasson, and M. Hirth, *Ozone: Science & Engineering* **10**, 12 (1988).